Taylor & Francis
Taylor & Francis Group

Phase Transitions
A Multinational Journal

ISSN: 0141-1594 (Print) 1029-0338 (Online) Journal homepage: http://www.tandfonline.com/loi/gpht20

Effect of La^{3+}-donor substitution on structural, micro structural, dielectric and ferroelectric characteristics of BLNT-BZT solid solutions

Karri Raju, Kumara Raja Kandula, Saket Asthana & Tirupathi Patri

To cite this article: Karri Raju, Kumara Raja Kandula, Saket Asthana & Tirupathi Patri (2018): Effect of La^{3+}-donor substitution on structural, micro structural, dielectric and ferroelectric characteristics of BLNT-BZT solid solutions, Phase Transitions, DOI: 10.1080/01411594.2018.1535065

To link to this article: https://doi.org/10.1080/01411594.2018.1535065

Published online: 26 Oct 2018.

PHASE TRANSITIONS
https://doi.org/10.1080/01411594.2018.1535065

Taylor & Francis
Taylor & Francis Group

Effect of La^{3+}-donor substitution on structural, micro structural, dielectric and ferroelectric characteristics of BLNT-BZT solid solutions

Karri Raju[a], Kumara Raja Kandula[b], Saket Asthana[b] and Tirupathi Patri[c]

[a]Department of Metallurgical & Materials Engineering, Rajiv Gandhi University of Knowledge Technologies, (AP-IIIT), RK Valley, India; [b]Advanced Functional Materials Laboratory, Department of Physics, Indian Institute of Technology Hyderabad, Sangareddy, India; [c]Department of Physics, Rajiv Gandhi University of Knowledge Technologies, (AP-IIIT), RK Valley, India

ABSTRACT

Lanthanum (La)-modified $0.93(Bi_{0.5-x}La_xNa_{0.5}TiO_3)$–$0.07(BaTi_{0.96}Zr_{0.04}O_3)$ ($0.00 \leq x \leq 0.08$) (Abbreviated as BLNT-BZT) ceramics were synthesized (close to MPB) by using conventional solid state route. The structural phase purity of ceramics was confirmed by using room temperature (RT) X-ray diffraction. The structural phases coexistence was analyzed with different duel phase model and bring out the amount of phase contribution quantitatively with the help of Rietveld refinement technique. The X-rays diffraction studies revealed that coexisting of minor tetragonal (P4mm) phase evolution along with major monoclinic structural (Cc) phase. Moreover, the above affirmation was clarified from Raman studies, observed that TiO_6 reflection at 500–600 cm^{-1} splitting occurs resides the presence of MPB of ceramics. With the substitution of La in BNT–BZT induces the gradual change in the average grain size and non-uniform distribution was observed from the surface morphology. The dielectric anomalies of these BLNT-BZT ceramics show broad dielectric anomaly near the maximum dielectric constant, which reflects the diffuse phase transition behavior. The RT P-E loops were observed in slim and slanted shape, replicates the enhanced properties due to the phase additive behavior near the MPB.

ARTICLE HISTORY
Received 9 August 2018
Accepted 4 October 2018

KEYWORDS
Ferroelectric; dielectric phase transitions; Cuires Weiss law; strcutural and microstructural; saturation polarization; tetragonal phase; antiferroelectrics

1. Introduction

Lead free ferroelectric materials are exhibits an important role in wide range of applications such as sensors, actuators, solid state lasers, ultrasonic transducers and high energy charge storage density devices due to their admirable ferro/piezoelectric properties [1–4]. Among all ferro/piezoelectric systems, lead zirconate titanate Pb (Zr_xTi_{1-x}) O_3 [PZT] is one of the most widely studied and used as functional ceramic down to excellent electromechanical properties [5]. However, PZT has excellent piezoelectric properties and suitable for many device applications but the prime concern is about non-eco-friendly lead (Pb), which creates a space for searching appropriate candidate to replace lead based system [6]. Recently, there have been many potential reports on lead-free ferro/piezoelectric ceramics, among all lead free bismuth sodium titanate ($Na_{0.5}Bi_{0.5}TiO_3$) (NBT) is the one of promising lead-free candidate owing its strong remnant polarization (P_r) ~38 μC/cm^2 and high curie temperature ~320°C [7,8]. It has simple perovskite (ABO_3) structure with low depolarization temperature (160–190°C). However, NBT exhibits high conductivity, large coercive field ~73 kV/cm

CONTACT Tirupathi Patri ptirupathi36@gmail.com

and poor piezoelectric coefficient (73–80 pC/N). A-site of this NBT shared by two different cations with different ionic radii and charge balance states [9,10].

To address the above affirmations in NBT, it's need to modify with site specific substituting at both A and B-site with similar valance and close ionic radii of different cations to improve its desired properties to wards PZT. However to enhancement these, desired properties in NBT, another useful method is the selection of different compositions near the morphotropic phase boundary (MPB) called as binary solid solutions, such as BNT–BT [11–13], BNT–BKT [14], BNT–ST [15] BNT–BST [16] and BNT–BZT [17]. The number of BNT-based binary systems showed improved piezoelectric and electromechanical properties near MPB region only. For instance, BNT–BT is one of the most well explored solid solution which posses MPB at (0.06 − 0.07). In the interim, Lee et al., also report a complete phase diagram of BNT–BST solid solutions. Similarly other perovskite system such as BNT–BKT ceramics exhibited MPB between rhombohedral to tetragonal at ($0.16 \leq x \leq 0.20$) also well studied.

In recent times, lead-free barium zirconium titanate Ba ($Zr_{1-x}Ti_x$) O_3 (BZT) also acquired great attraction due to its attractive dielectric and ferroelectric properties; those are suitable for capacitor applications. The substitution of Zr^{4+} into $BaTiO_3$ shifted the Curie temperature (T_c) from 130°C to towards room temperature and achieves a high dielectric constant with low dielectric loss. Lateron, Peng.C et al., studied the substitution of $Ba(Zr_{1-x}Ti_x)O_3$ into $(Bi_{0.5}Na_{0.5})TiO_3$ (i.e. BNT-BZT) and observed with an enhancement in dielectric and piezoelectric properties at close to MPB of $x = 0.080$ [18]. Keep in this view, we examined the effect of La^{3+} substitution on NBT-BZT solid solutions near at MPB with help of nominal formula $0.93[(Bi_{0.5-x}La_xNa_{0.5})TiO_3]$–$0.07[Ba(Zr_{0.04}Ti_{0.96})O_3]$ ($0.0 \leq x \leq 0.08$). The effect of La^{3+} substitution on structural phase transitions; microstructure, ferroelectric and dielectric properties were investigated and discussed in detail.

2. Experimental

The lead free ceramics $0.93(Bi_{0.5-x}La_xNa_{0.5}TiO_3)$–$0.07(BaTi_{0.96}Zr_{0.04}O_3)$ [BLNT-BZT] ($0.00 \leq x \leq 0.08$) were synthesized with the help of conventional solid-state reaction route by using high – purity (≥ 99.9%) ingredients: Bi_2O_3, La_2O_3, Na_2CO_3, $BaCO_3$, ZrO_2, and TiO_2 taken into stoichiometric ratio and mixed thoroughly in agate mortar in Iso-propanal (IPA) medium. All these materials are mixed together thoroughly and mixtures were calcined at 600°C for 5h and 1050°C for 6h subsequently. The primary calcination helps to remove volatile, gaseous and unwanted materials from the powder and later one is used to achieve the desired crystal phase and particle size. The structural phase purity confirmed with the help of X-ray diffraction (XRD) technique (PHILIPS, PW3373 XPERT-PRO). The structural phase coexistence resolved by adopting Rietveld refinement method (Fullprof software 2000). Finally, the calcined powders were compact into a circular disc of diameter (Ø = 10 mm) and thickness 1–2 mm under a hydrostatic pressure of about 12×10^6 N/m^2 by using a hydraulic press. The pellets were sintered in a covered alumina crucible in air atmosphere at 1100°C for 6h. The temperature dependence dielectric measurements were performed on silver electrode ceramics with wide temperature range 30–400° C with a frequency range 5 KHz to 1 MHz by using (Wayne Kerr 6500B) impedance analyzer. The surface morphology of BLNT-BZT ceramics were checked by using SEM (Carl Zeiss, Supra 40). The room temperature polarization (P) vs electric field (E) measurements were performed using TF-Analyzer 2000 (aix ACCT systems, GmbH) on the silver-coated samples.

3. Results and discussion

3.1. Structural phase transitions

The room temperature X-ray diffraction (XRD) pattern of La modified BLNT-BZT ceramics are shown in Figure 1(a). All ceramics shows pure in phase and crystallinity nature, which deserves as stabilizing in perovskite structure without coexisting of secondary phases. It is worth to notice

that the peak positions are shifted towards higher angle side with substitution of La^{3+} at particular Bi-site throughout the series, which can be attributed due to the mismatch of ionic radii of La^{3+} (1.03Å) compared to Bi^{3+} (1.37Å). In order to provide visual clarity to explore the evolution of structural phase over compositional dependent along with major structural phase of Cc, only particular pseudo cubic Bragg reflection of $(-222)_{pc}$ have been shown on the enlarged scale $(46^{\circ} \leq 2\theta \leq 47^{\circ})$ in Figure 1(b). It is clearly shown with increasing La^{3+} donor substitution the peak $(-222)_{pc}$ exhibiting a splitting of the $(200)_{pc}/(-222)_{pc}$ diffraction peaks up to $x = 0.08$ composition, which it confirms coexistence of dual phase.

To identify the structural phase transformation of all these ceramics, the XRD peaks at particular angle (2θ) between 46–47° and 57–58° were de convoluted by using Gaussian –Lorentzian peak fit with help of origin software [19] (as shown in Figure 2(a,b)). The de-convolution of $(-222)_{pc}/(200)_{pc}$ at 46–47° angle and $(202)_{pc}/(131)_{pc}$ peak profile at 57–58° is identifies the evaluation secondary phase. With Further increases x, the peak $(200)_{pc}$ tends splits the splitting becomes more and more obvious, suggesting that a new secondary phase might present up to $x \leq 0.08$. In order to explore the possibility of coexisting structural phases contribution of these ceramics near the MPB region $(0.00 \leq x \leq 0.08)$, we consider multiple space group including R3c, P4bm, Pm3m, P4mm, Cc and Cm to model it. It is well reported that, room temperature structure of BNT has been argued to possess a stable rhombhohedral structure with R3c space group [20,21]. Keeping this in mind, we started considering R3c space group initially to investigate crystal system, however the R3c model provides a rationally good quality of fit ($R_p = 9.45\%$), the calculated pattern for (110) and (111) multiple reflections in the R3c model deviates from the observed pattern in at maximum intensities. Recently, X. Liu et al., reported a systematic study on La doped BNBT ceramics with help of transmission electron microscopy suggests the presence of minor tetragonal phase along with rhombohedral [19,22]. Therefore, we modeled with R3c + P4bm, R3c + P4mm *etc* … other mixed phase systems which were not given the satisfactory results. Later on, we modeled with Cc space groups, where Cc is a subgroup of the R3c space group. Therefore, we tried with Cc space group for $x = 0.00$, fitted with monoclinic structure (Cc space group) shown in Figure 3(a). The noted reliability factors for $x = 0.00$ ceramics with pure monoclinic structure is $R_p = 9.04$ $R_{wp} = 6.15$ and $\chi^2 = 5.63$ and lattice constant are $a = 9.5540$ (Å), $b = 5.5199$ (Å), $c = 5.5075$ (Å) and $v = 237.0057$ Å^3. Even though there is a mismatch at the higher angle region shown inset Figure 3(a) and observed fitting parameters suggest that refinement results are not reliable. Furthermore, the refinement has been performed by add secondary phase tetragonal (P4mm) to monoclinic (Cc) model to confirm the nature of additional phase.

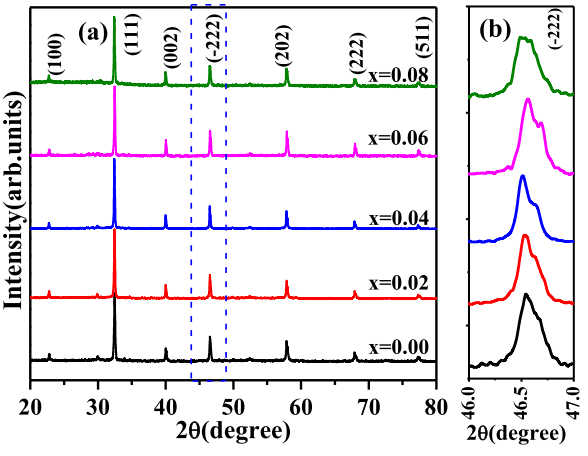

Figure 1. (a) Powder X-ray diffraction patterns of La modified $0.93(Bi_{0.5-x}La_xNa_{0.5}TiO_3)$–0.07 $(Ba\ Ti_{0.96}\ Zr_{0.04}O_3)$ $(0.0 \leq x \leq 0.08)$. (b) Main intense peak $(110)_{PC}$ peak shifting towards higher angle shown inset.

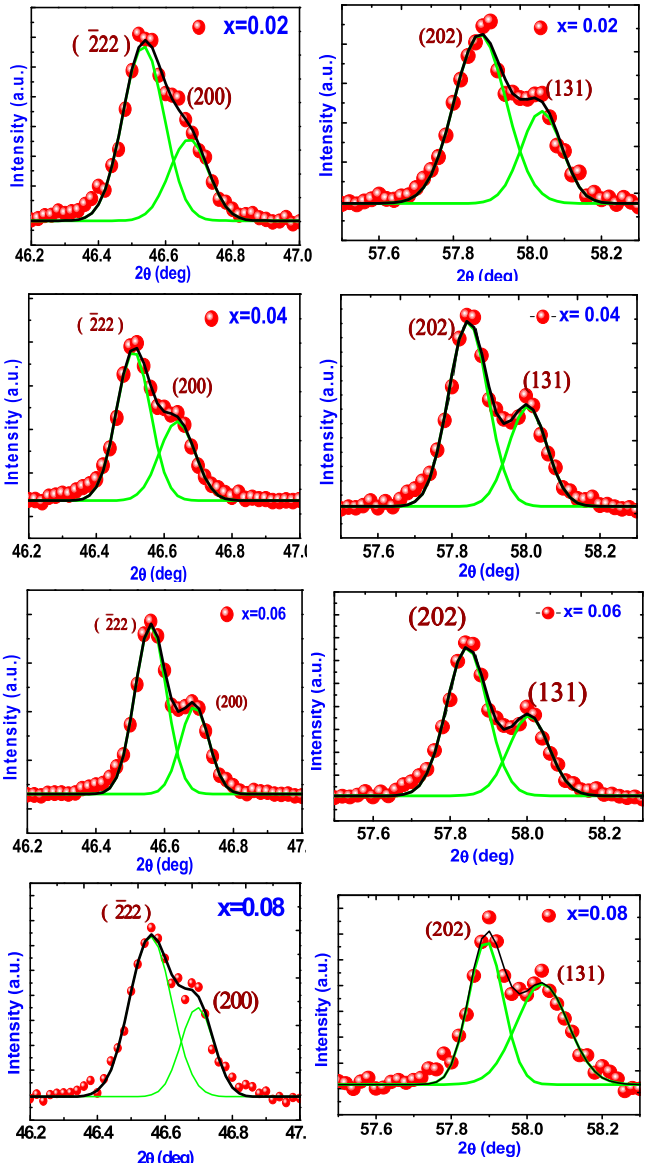

Figure 2. De-convolution of (002)/(−222)$_{pc}$ peak at an angle 46–47°region and (202)$_{pc}$/(103)pc at 57–58° peak profile to identify the evaluation of secondary phase.

Evidently, it is well fitted with mixed phase Cc + P4mm of acceptable reliable factors shown in Figure 3(b).

For $x = 0.02$ onwards, the observed extra peak (Blue color) identified as a tetragonal reflection of (200)$_{pc}$ after deconvolution (Shown in Figure 2(a)), is formerly considered two-phase models-Cc + P4mm up to x~0.08 composition. The results obtained from the Rietveld refinement show good agreement between the measured experimental XRD patterns. Where the contribution of tetragonal (P4mm) phase is pronounced with little in the account, compared to pure $x = 0.00$. Figure 4 (a–d) shows Rietveld refined plots of La^{3+} substituted BLNT-BZT ceramics $0.02 \leq x \leq 0.08$. The zoomed pattern of particular (200)$_{pc}$/(−222)$_{pc}$ peaks is also represented inset of Figure 4(a–d). The refined lattice parameters and reliable constants are good agreement with recent potential reports is

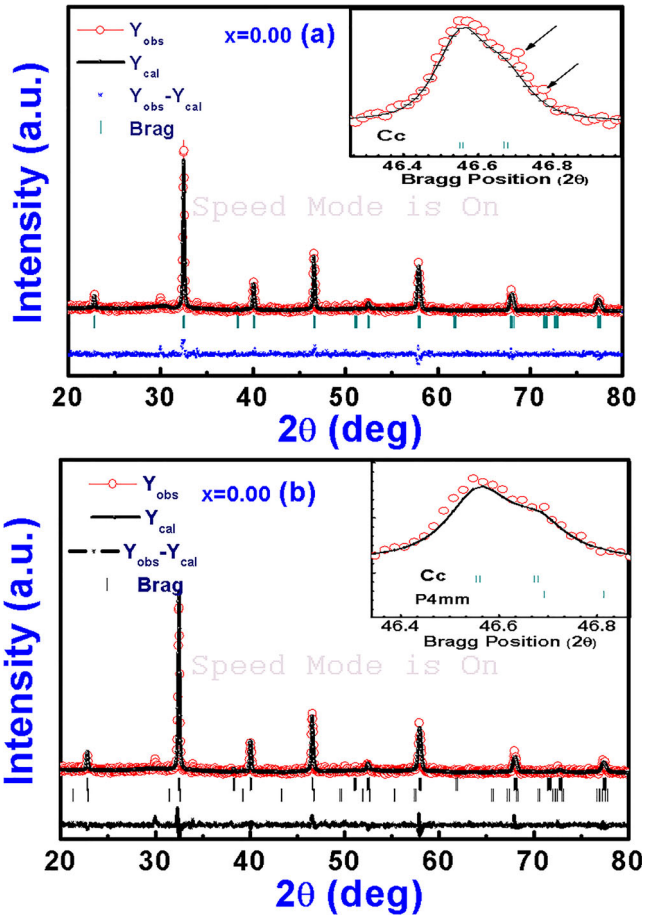

Figure 3. Rietveld refinement pattern of pure BLNT-BZT ceramics at (a) $x = 0.00$, with monoclinic Cc phase model and (b) $x = 0.00$, Cc + P4mm mixed phase model. The insets highlight the enlarged view in the region 46–47°.

shown in Table 1 [20]. Henceforth, it can conclude that the ceramics have been residing MPB near to compositions $0.00 \leq x \leq 0.08$, further it was confirmed by Raman spectroscopy studies.

3.2. Raman spectroscopy analysis

Raman spectroscopy is an effective tool for identifying the structural modification and lattice vibrations of the crystals. In order to identify the functional groups in present ceramics, we carried room temperature Raman measurements on the smooth surface of sintered ceramics to avoid the scattering effects. Raman modes are mainly occurring due to the internal vibrations of lattice point in octahedral/ tetrahedral sites [21,23–25]. Here, the Raman spectra of La^{3+} substituted BLNT-BZT ceramics are shown in two regions; 60–180 cm^{-1} denoted as Region-I and 200–900 cm^{-1} denoted as Region-II in Figure 5(a,b). The complete spectrum of the ceramics clearly represents a broad signature of induced relaxor activity due to A-site disorder in perovskites structure. In Region-I, it was observed three Raman modes i.e. 79, 117 and 132 cm^{-1} respectively, which related to vibrations of the Bi-O and Na-O bonds. Beside this, we noted the softening of Raman modes with La^{3+} compositional dependent, which it reveals that produce internal strain due to mismatch of ionic radii of La^{3+} and Bi^{3+} at A-site. In Region-II there are five Raman active modes were observed i.e. 214, 292, 541, 601 and 812 cm^{-1} respectively. All these are attributed to internal stretching and

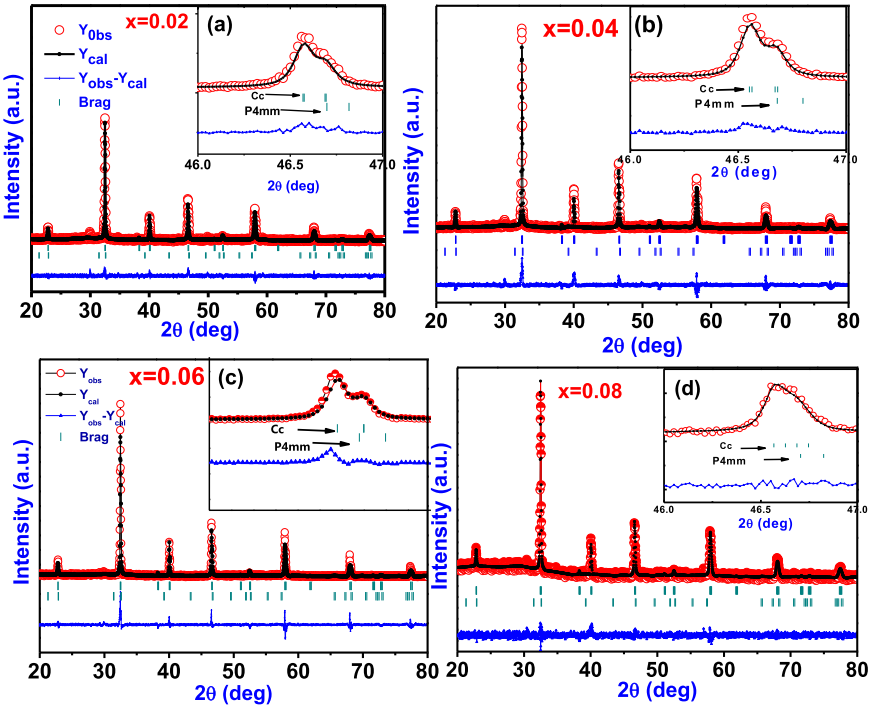

Figure 4. Rietveld refinement plots of BLNT-BZT ceramics ($0.02 \leq x \leq 0.08$) (a) $x = 0.02$, (b) $x = 0.04$, (c) $x = 0.06$, (d) $x = 0.08$, with Cc + P4mm coexistence of two phase model. The insets highlight the enlarged view in the region 46–47° of corresponding ceramics with Cc + P4mm Bragg profile.

bending vibrations of Ti-O bond in TiO_6 octahedral [26]. A special splitting of two bands was observed in between 541 and 601 cm^{-1} indicates coexistence of dual phase between monoclinic to tetragonal thus this confirm residing of MPB in present ceramics.

Table 1. Comparison of Rietveld refined lattice parameters, phase factors, angles, calculated grain size, observed dielectric constant and phase transition temperatures (T_d and T_m).

Parameters	$x = 0.00$	$x = 0.02$	$x = 0.04$	$x = 0.06$	$x = 0.08$
Lattice parameters(Å)	$a = 9.5487$	$a = 9.5530$	$a = 9.5430$	$a = 9.5425$	$a = 9.5419$
Cc space group	$b = 5.5102$	$b = 5.5089$	$b = 5.5072$	$b = 5.5060$	$b = 5.5091$
Angles (°)	$c = 5.5117$	$c = 5.5180$	$c = 5.5109$	$c = 5.5176$	$c = 5.5113$
	$\alpha = \beta = 90°$,	$\alpha = \beta = 90°$,	$\alpha = \beta = 90°$,	$\alpha = \beta = 90°$,	$\alpha = \beta = 90°$,
	$\gamma = 125.23°$	$\gamma = 125.31°$	$\gamma = 125.32°$	$\gamma = 125.32°$	$\gamma = 125.34°$
Lattice parameters(Å)	$a = b = 3.8871$	$a = b = 3.8885$	$a = b = 3.8874$	$a = b = 3.8866$	$a = b = 3.8886$
P4mm space group	$c = 4.1739$	$c = 4.1772$	$c = 4.1722$	$c = 4.1743$	$c = 4.1764$
Angles (°)	$\alpha = \beta = \gamma = 90°$	$\alpha = \beta = \gamma = 90°$	$\alpha = \beta = \gamma = 90°$	$\alpha = \beta = \gamma = 90°$	$\alpha = \beta = \gamma = 90°$
Avg. Grain size(μm)	1.41	1.22	0.91	0.87	0.67
Dielectric constant (ε) (at 50 kHz) at T_m	2114	2263	6505	1044	845
Depolarization temperature(T_d)	118°C	115°C	113°C	108°C	100°C
Temperature at (ε)maxi(T_m)	310°C	298°C	287°C	285°C	260°C
Dielectric constant at RT @ 50 kHz	813	888	364	664	605
Percentage of phase fractions (Cc+P4mm)	(99.86 + 0.14)	(99.84 + 0.16)	(99.67 + 0.33)	(99.55 + 0.45)	(99.52 + 0.48)
RT Energy density (J/cm^3)	0.86	0.73	0.61	0.92	0.95

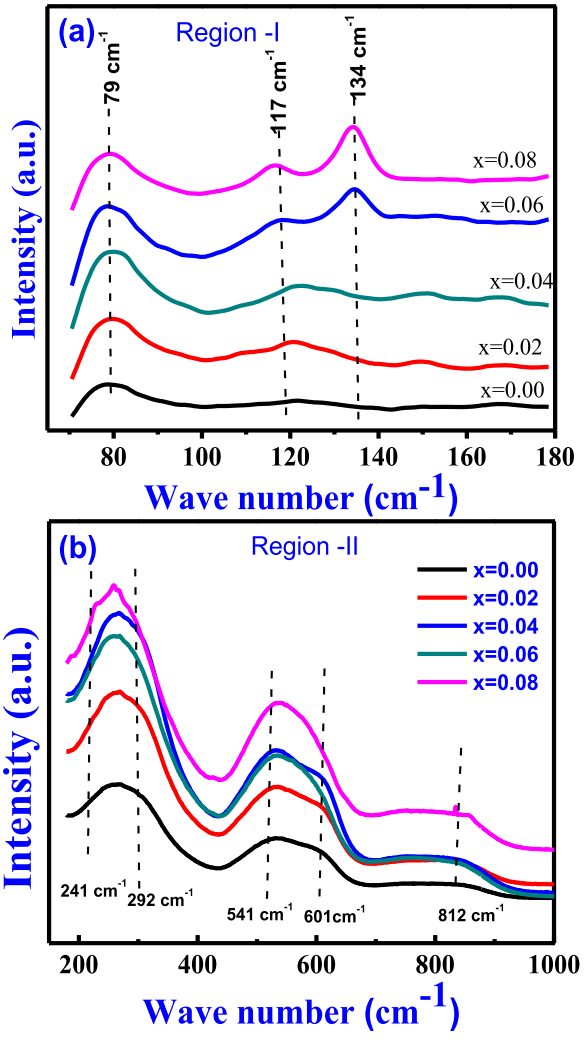

Figure 5. Raman spectrum of BLNT-BNT ceramics of ($0.00 \leq x \leq 0.08$) (a); Region-I in between 100 and 180 cm^{-1} (b); Region-II in between 200 and 900 cm^{-1}.

3.3. Micro structural analysis

The surface micrographs of the BLNT-BZT ceramics are shown in Figure 6(a). It is found that pure ceramic $x = 0.00$, shows uniform grains without any intragranular pores. The La^{3+} donor dopant in BNT-BZT leads to the slight change in grain size, nonuniform grain growth and increase in porosity. The observed average grain sizes are 1.41, 1.21, 1.02, 0.91 and 0.87 μm for $x = 0.00,\ 0.02,\ 0.04,\ 0.06$ and 0.08 respectively, which it show decreasing of grain size with increasing La-donor dopant. The substitution of La suppresses grain growth and non-uniformity increases. The non-uniformity and decreasing in grain size might be attributed due to the various sizes of the starting powders those have different priorities to sit different ionic radii at A-site La^{3+}, replaces with Na^{+} in the sintering process. Further at large La^{3+} donor substitution will lead to an inhibition of grain growth $x \geq 0.4$.

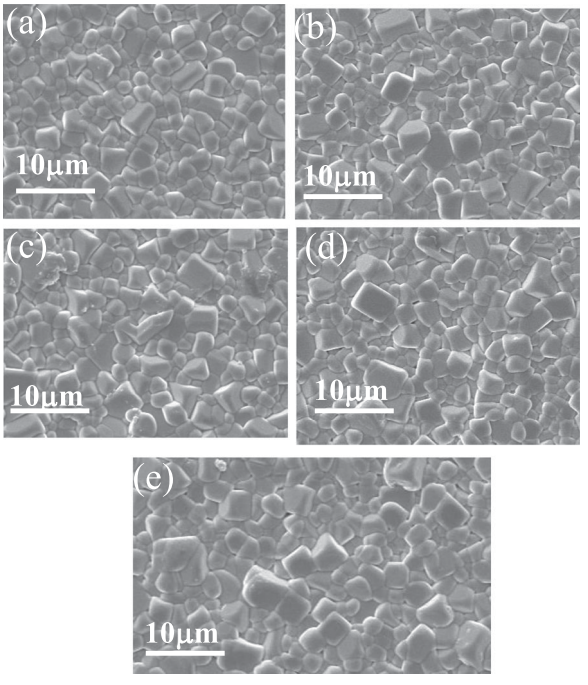

Figure 6. SEM micrographs of the fractured surface of BLNT-BZT ceramics. (a) $x = 0.00$, (b) $x = 0.02$, (c) $x = 0.04$, (d) $x = 0.06$, (e) $x = 0.08$.

3.4. Dielectric analysis

To investigate the structural phase transition behaviour of these ceramics near MPB region, we performed temperature-dependence of the relative permittivity (ε_r) and dielectric loss (tanδ) of BLNT-BZT ($0.00 \leq x \leq 0.08$) at wide range frequencies (5 KHz to 1 MHz) over the wide temperatures (30–450°C). All the ceramics exhibited two dielectric phase transition peaks around 100°C and 300°C, over the wide temperature of dielectric mesurement. In Figure 7(a–e) the transition temperatures T_d (depolarization temperature) & T_m (maximum temperature), are shown thought the series. In each specimen, we observed two dielectric anomalies from the dielectric vs temperature curves. The first anomaly corresponds to the T_d, which is responsible for the FE and AFE transition. The second anomaly corresponds to T_m which is responsible for AFE to PE transition. The noted phase transition temperatures and corresponding dielectric constant values were listed in Table 1. It is found that the dielectric constant increases with increasing La content become maxima at $x = 0.04$, then starts to decreases up to $x = 0.08$. Whereas the prominent dielectric maximum of ~2114 at ratio $x = 0.00$ increases to 6605 at $x = 0.04$ composition reaches maximum and then starts to decreases to 845 at $x = 0.08$ composition. This could be explained by considering the concept of free energy of monoclinic phase was close to the tetragonal phase. These two phases are present for $x = 0.04$ compositions in BLNT-BZT ceramics, which are more favor and easily changed to each other when they wee subjected to an applied electric fields. This helps to promote the movement and polarization of ferroelectric active ions, leading to the increase of dielectric constant. And further substitution of La ($x > 0.04$), leads to decrease in tetragonal phase reflections in monoclinic Cc phase causes to decreasing in dielectric constant [27].

On the other hand, the observed phase transition temperatures T_d and T_m are decreases from 118°C to 100°C and 310°C to 260°C respectively as La concentration increases from $x = 0.00$ to 0.08. The decreasing of T_d and T_m phase transitions mainly due to the structural distortion that pronounced of non-cubic phase with incorporation of La^{3+} into BNT–BZT ceramics. As a result the coexistence

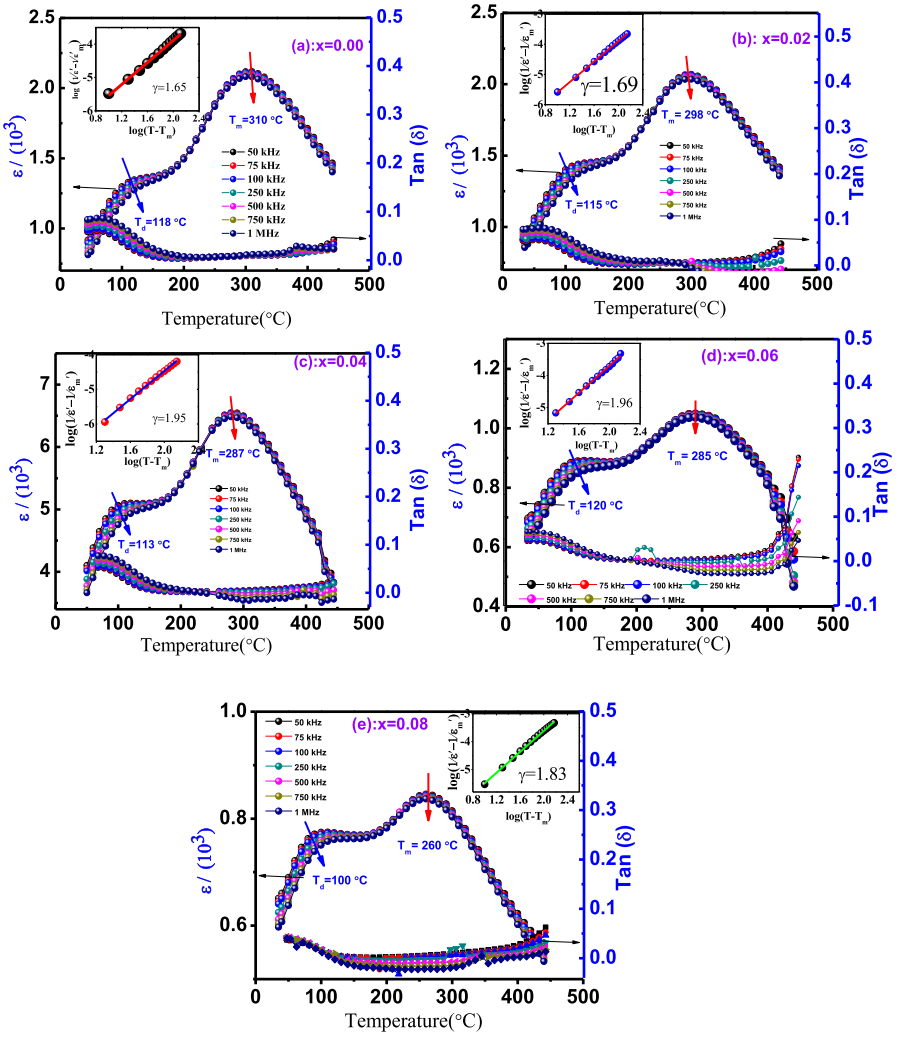

Figure 7. Temperature-dependence dielectric permittivity and loss of BLNT–BZT ceramics in the region of 30–450°C at frequencies of (50, 75, 100, 250, 500, 750 and 1000 KHz) (a) $x = 0.00$, (b) $x = 0.02$, (c) $x = 0.04$, (d) $x = 0.06$ and (e) $x = 0.08$. Inset figure shows the modified Curie-Weiss law fitting of corresponding samples.

of a mixed phase could lead to more powerful stress in the MPB compositions, due to the incompatibility of their structural domain, resulting in decrease of the thermal stability leads to the destabilization of ferroelectric order [28,29]. The present results and observed dielectric phase transitions of the ceramics are well agreed with recent reports [30]. With increasing of La concentration gradually broadened the dielectric anomalies at T_m suggesting that La concentration induces a diffuse phase transition in the ceramics. To identify the observed diffuse phase transition behavior or disorderness of these ceramics, we analyzed with the help of modified Curie–Weiss law: $1/\varepsilon' - 1/\varepsilon'_m = (T - T_m)^{\gamma}/C$. The estimated diffusion coefficient (γ) values at frequency of 50 KHz for all ceramics were shown in the inset of Figure 7 respectively. It is found that diffusion coefficient (γ) of these ceramics were increases with La concentration. The diffused transformation might be the presence of complex cations at A-site in the compositions of the ceramics. Thus, it is an evidence transition from ferroelectric (FE) to non-polar (NP) state as a function of La concentration. The observed dielectric loss values were very low at temperatures below 350°C and almost constant for all these compositions with negligible dispersion.

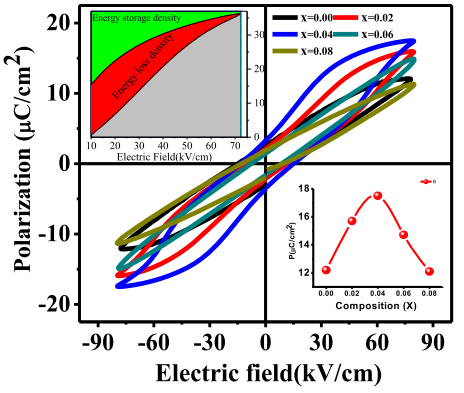

Figure 8. Room temperature P-E loops observed at 1Hz loop frequency of BLNT-BZT ceramic. Inset figure shows schematic representation of energy density and energy loss values.

However, it increased at temperatures above 350°C which may be due to the thermally activated conduction charge carriers [31]. The dielectric loss is usually attributed to space charges which exist in BNT based composition with A-site deficiency serving as charged vacancies are created during high temperature sintering.

4. Polarization studies

The effect of La^{3+} substitution on ferroelectric properties is illustrated in P-E studies. In Figure 8 shows the polarizations vs electric field loops are characterize at a frequency of 1Hz. The pure BNT-BZT ceramic has slim hysteresis loop like soft ferroelectrics character with saturation polarization ($P_s = 12.2$ μC/cm^2). With increasing La^{3+} concentration in BNT-BZT ceramics increase in polarization (17.5 μC/cm^2) value up to $x = 0.04$ were observed. Further substitution ($x \geq 0.04$) saturation polarization (P_s) and slated slim hysteresis reduced progressively which are shown in Figure 8. It indicates that ferroelectric properties of BLNT-BZT ceramics are declining as the incorporation of La^{3+} with high substitution $x > 0.04$. This is well coordination or good agreement with the XRD analysis. Generally, the tetragonal phase shows antiferroelectric characteristics while monoclinic phase shows ferroelectric characteristics of NBT-based materials. The coexistence of monoclinic and tetragonal indicates the disruption of the long FE domains, so these ceramics were transformed from ferroelectric phase to antiferroelectric phase gradually with substitution of La^{3+}; it leads to slim asymmetric hysteresis loops. Such slim and slanted ferroelectric materials have capable for high storage energy density rather than normal ferroelectric [18,22]; henceforth, these materials will be useful for future energy storage device applications. The estimated energy storage values from the upper branch of the polarization loops are listed in the Table 1. The schematic view of the area representation belongings to storage and loss can be identifying inset of Figure 8.

5. Conclusions

In summary, we successfully synthesized BLNT-BZT ($0.00 \leq x \leq 0.08$) close to morph-tropic phase boundary by using solid state reaction route. The structural phase coexistence analyzed quantitatively with the help of Rietveld refinement technique reveals the coexistence of mixed phase i.e. major monoclinic (Cc) to minor tetragonal (P4mm) phase up to $x \sim 0.08$. Raman spectroscopy studies also supports, structural modifications in MPB region observed $x = 0.00$ to $x = 0.08$ compositions. The temperature and frequency dependence dielectric studies confirm the La substitution induces the ferroelectric to diffuse dielectric (non-polar) (FE-NP) phase transitions. The substitution

of La^{3+} leads to slim asymmetric P-E loops observed in polarization studies. Hence, we can conclude that the material La modified NBT-BZT ceramics are promising candidates for future energy storage device applications.

Disclosure statement

No potential conflict of interest was reported by the authors.

References

[1] Benes E, Gröschl M, Burger W, et al. Sensors based on piezoelectric resonators. Sens Actuat A-Phys. 1995;48 (1):1–21.

[2] Kandula KR, Banerjee K, Raavi SS, et al. Enhanced electrocaloric effect and energy storage density of Nd-substituted 0.92 NBT-0.08BT lead free ceramic. Phys Status Solidi A. 2018;215(7):1700915.

[3] Kandula KR, Raavi SS, Asthana S. Correlation between structural, ferroelectric and luminescence properties through compositional dependence of Nd^{3+} ion in lead free $Na_{0.5}Bi_{0.5}TiO_3$. J Alloy Compd. 2018;732:233–239.

[4] Kandula KR, Raavi SS, Asthana S. Enhancement in the structural, electrical and optical properties by substitution of lanthanides (Nd^{3+} and Eu^{3+}) in lead free $Na_{0.5}Bi_{0.5}TiO_3$ ceramics. Ferroelectrics. 2017;518(1): 23–30.

[5] Zhang S, Shrout TR, Nagata H, et al. Piezoelectric properties in $K_{0.5}Bi_{0.5}TiO_3$-$Na_{0.5}Bi_{0.5}TiO_3$-$BaTiO_3$ lead-free ceramics. IEEE Trans Ultrason Ferroelectr Freq Control. 2014;54(5):910–917.

[6] Kanno I, Fujii S, Kamada T, et al. Piezoelectric properties of c-axis oriented Pb (Zr, Ti) O_3 thin films. Appl Phys Lett. 1997;70(11):1378–1380.

[7] Thirupathi G, Kandula KR, Raavi SS, et al. The effect on electrical and luminescent properties in nanocrystalline $Na_{0.5}Bi_{0.5-x}Nd_xTiO_3$. Mater Res Express. 2017;4(9):095019.

[8] Niranjan MK, Karthik T, Asthana S, et al. Theoretical and experimental investigation of Raman modes, ferroelectric and dielectric properties of relaxor $Na_{0.5}Bi_{0.5}TiO_3$. J Appl Phys. 2013;113(19):194106.

[9] Hiruma Y, Nagata H, Takenaka T. Thermal depoling process and piezoelectric properties of bismuth sodium titanate ceramics. J Appl Phys. 2009;105(8):084112.

[10] Takenaka T, Maruyama KI, Sakata K. $Na_{0.5}Bi_{0.5}TiO_3$-$BaTiO_3$ system for lead-free piezoelectric ceramics. Jpn J Appl Phys. 1991;30(9S):2236.

[11] Kandula KR, Raavi SS, Asthana S. Improved electrical and photoluminescence properties in Nd substitution of $0.94(Na_{0.5}Bi_{0.5}TiO_3)$-$0.06BaTiO_3$ lead free multi-functional ceramics. Adv Mater Lett. 2018;9(9):656–659.

[12] Zuo R, Ye C, Fang X, et al. Tantalum doped 0.94 Bi0. 5Na0. 5TiO3–0.06 BaTiO3 piezoelectric ceramics. J Eur Ceram Soc. 2008;28(4):871–877.

[13] Ullah A, Ullah A, Kim IW, et al. Large electromechanical response in lead free La-doped BNKT–BST piezoelectric ceramics. J Am Ceram Soc. 2014;97(8):2471–2478.

[14] Elkechai O, Manier M, Mercurio JP. $Na_{0.5}Bi_{0.5}TiO_3$– $K_{0.5}Bi_{0.5}TiO_3$ (NBT-KBT) system: a structural and electrical study. Phys Status Solidi A. 1996;157(2):499–506.

[15] Hiruma Y, Imai Y, Watanabe Y, et al. Large electrostrain near the phase transition temperature of $Na_{0.5}Bi_{0.5}TiO_3$–$SrTiO_3$ ferroelectric ceramics. Appl Phys Lett. 2008;92(26):262904.

[16] Peng C, Li JF, Gong W. Preparation and properties of $Na_{0.5}Bi_{0.5}TiO_3$–Ba(Ti, Zr)O_3 lead-free piezoelectric ceramics. Mater Lett. 2005;59(12):1576–1580.

[17] Kantha P, Pengpat K, Jarupoom P, et al. Phase formation and electrical properties of BNLT–BZT lead-free piezoelectric ceramic system. Curr Appl Phys. 2009;9(2):460–466.

[18] Wylie-van Eerd B, Damjanovic D, Klein N, et al. Structural complexity of $Na_{0.5}Bi_{0.5}TiO_3$-$BaTiO_3$ as revealed by Raman spectroscopy. Phys Rev B. 2010;82(10):104112.

[19] Liu X, Guo H, Tan X. Evolution of structure and electrical properties with lanthanum content in $[(Bi_{1/2}Na_{1/2})0.95Ba_{0.05}]$ 1− xLaxTiO$_3$ ceramics. J Eur Ceram Soc. 2014;34(12):2997–3006.

[20] Ma C, Guo H, Beckman SP, et al. Creation and destruction of morphotropic phase boundaries through electrical poling: a case study of lead-free $(Bi_{1/2}Na_{1/2})TiO_3$−$BaTiO_3$ piezoelectrics. Phys Rev Lett. 2012;109(10):107602.

[21] Jo W, Daniels JE, Jones JL, et al. Evolving morphotropic phase boundary in lead-free $(Bi_{1/2}Na_{1/2})TiO_3$–$BaTiO_3$ piezoceramics. J Appl Phys. 2011;109(1):014110.

[22] Herabut A, Safari A. Processing and electromechanical properties of $(Bi_{0.5}Na_{0.5})$(1− 1.5 x) LaxTiO$_3$ ceramics. J Am Ceram Soc. 1997;80(11):2954–2958.

[23] Kandula KR, Beanerjee K, Raavi SS, et al. A lead free 0.96 $(Na_{0.5}Bi_{0.49}Nd_{0.01}TiO_3)$-$0.04BaTiO_3$ piezoceramic for possible optoelectronic device applications. In AIP Conference Proceedings 2018, 1942, 030011.

[24] Yanamandra R, Kandula KR, Bandi P, et al. Enhanced energy storage density in lead free $(Na_{0.5}Bi_{0.48}Eu_{0.02})$ $Ti_{1-x}NbxO_3$(x=0.00,0.01&0.02) ceramics. InAIP Conference Proceedings 2018, 1953, 050063.

[25] Zhang Y, Hao J, Mak CL, et al. Effects of site substitutions and concentration on upconversion luminescence of Er^{3+}-doped perovskite titanate. Opt Express. 2011;19(3):1824–1829.
[26] Chen ZW, Hu JQ. Piezoelectric and dielectric properties of $Bi_{0.5}$ $(Na_{0.84}K_{0.16})0.5TiO_3$–Ba $(Zr_{0.04}Ti_{0.96})O_3$ lead free piezoelectric ceramics. Adv Appl Ceram. 2008;107(4):222–226.
[27] Kandula KR, Asthana S, Raavi SS. Multifunctional Nd^{3+} substituted $Na_{0.5}Bi_{0.5}TiO_3$as lead-free ceramics with enhanced luminescence, ferroelectric and energy harvesting properties. RSC Adv. 2018;8(28):15282–15289.
[28] Smolensky GA. New ferroelectrics of complex composition. IV. Sov Phys Solid State. 1961;2:2651–2654.
[29] Jaita P, Watcharapasorn A, Jiansirisomboon S. Investigation of a new lead-free $Bi_{0.5}$ $(Na_{0.40}$ $K_{0.10})$ TiO_3-$(Ba_{0.7}Sr_{0.3})$ TiO_3 piezoelectric ceramic. Nanoscale Res Lett. 2012;7(1):24.
[30] Singh A, Chatterjee R. Structural, electrical, and strain properties of stoichiometric $1- x- y(Bi_{0.5}Na_{0.5})TiO_3-x$ $(Bi_{0.5}K_{0.5}TiO_3)- y(Na_{0.5}K_{0.5})NbO_3$ solid solutions. J Appl Phys. 2011;109(2):024105.
[31] Ahn CW, Kim HS, Woo WS, et al. Low-temperature sintering of $Bi_{0.5}(Na,K)_{0.5}TiO_3$ for multilayer ceramic actuators. J Am Ceram Soc. 2015;98(6):1877–1883.